LETTER

doi:10.1038/nature12914

Rate of tree carbon accumulation increases continuously with tree size

N. L. Stephenson[1], A. J. Das[1], R. Condit[2], S. E. Russo[3], P. J. Baker[4], N. G. Beckman[3]†, D. A. Coomes[5], E. R. Lines[6], W. K. Morris[7], N. Rüger[2,8]†, E. Álvarez[9], C. Blundo[10], S. Bunyavejchewin[11], G. Chuyong[12], S. J. Davies[13], Á. Duque[14], C. N. Ewango[15], O. Flores[16], J. F. Franklin[17], H. R. Grau[10], Z. Hao[18], M. E. Harmon[19], S. P. Hubbell[2,20], D. Kenfack[13], Y. Lin[21], J.-R. Makana[15], A. Malizia[10], L. R. Malizia[22], R. J. Pabst[19], N. Pongpattananurak[23], S.-H. Su[24], I-F. Sun[25], S. Tan[26], D. Thomas[27], P. J. van Mantgem[28], X. Wang[18], S. K. Wiser[29] & M. A. Zavala[30]

Forests are major components of the global carbon cycle, providing substantial feedback to atmospheric greenhouse gas concentrations[1]. Our ability to understand and predict changes in the forest carbon cycle—particularly net primary productivity and carbon storage—increasingly relies on models that represent biological processes across several scales of biological organization, from tree leaves to forest stands[2,3]. Yet, despite advances in our understanding of productivity at the scales of leaves and stands, no consensus exists about the nature of productivity at the scale of the individual tree[4–7], in part because we lack a broad empirical assessment of whether rates of absolute tree mass growth (and thus carbon accumulation) decrease, remain constant, or increase as trees increase in size and age. Here we present a global analysis of 403 tropical and temperate tree species, showing that for most species mass growth rate increases continuously with tree size. Thus, large, old trees do not act simply as senescent carbon reservoirs but actively fix large amounts of carbon compared to smaller trees; at the extreme, a single big tree can add the same amount of carbon to the forest within a year as is contained in an entire mid-sized tree. The apparent paradoxes of individual tree growth increasing with tree size despite declining leaf-level[8–10] and stand-level[10] productivity can be explained, respectively, by increases in a tree's total leaf area that outpace declines in productivity per unit of leaf area and, among other factors, age-related reductions in population density. Our results resolve conflicting assumptions about the nature of tree growth, inform efforts to understand and model forest carbon dynamics, and have additional implications for theories of resource allocation[11] and plant senescence[12].

A widely held assumption is that after an initial period of increasing growth, the mass growth rate of individual trees declines with increasing tree size[4,5,13–16]. Although the results of a few single-species studies have been consistent with this assumption[15], the bulk of evidence cited in support of declining growth is not based on measurements of individual tree mass growth. Instead, much of the cited evidence documents either the well-known age-related decline in net primary productivity (hereafter 'productivity') of even-aged forest stands[10] (in which the trees are all of a similar age) or size-related declines in the rate of mass gain per unit leaf area (or unit leaf mass)[8–10], with the implicit assumption that declines at these scales must also apply at the scale of the individual tree. Declining tree growth is also sometimes inferred from life-history theory to be a necessary corollary of increasing resource allocation to reproduction[11,16]. On the other hand, metabolic scaling theory predicts that mass growth rate should increase continuously with tree size[6], and this prediction has also received empirical support from a few site-specific studies[6,7]. Thus, we are confronted with two conflicting generalizations about the fundamental nature of tree growth, but lack a global assessment that would allow us to distinguish clearly between them.

To fill this gap, we conducted a global analysis in which we directly estimated mass growth rates from repeated measurements of 673,046 trees belonging to 403 tropical, subtropical and temperate tree species, spanning every forested continent. Tree growth rate was modelled as a function of log(tree mass) using piecewise regression, where the independent variable was divided into one to four bins. Conjoined line segments were fitted across the bins (Fig. 1).

For all continents, aboveground tree mass growth rates (and, hence, rates of carbon gain) for most species increased continuously with tree mass (size) (Fig. 2). The rate of mass gain increased with tree mass in each model bin for 87% of species, and increased in the bin that included the largest trees for 97% of species; the majority of increases were statistically significant (Table 1, Extended Data Fig. 1 and Supplementary Table 1). Even when we restricted our analysis to species achieving the largest sizes (maximum trunk diameter >100 cm; 33% of species), 94% had increasing mass growth rates in the bin that included the largest trees. We found no clear taxonomic or geographic patterns among the 3% of species with declining growth rates in their largest trees, although the small number of these species (thirteen) hampers inference. Declining species included both angiosperms and gymnosperms in seven of the 76 families in our study; most of the seven families had only one or two declining species and no family was dominated by declining species (Supplementary Table 1).

When we log-transformed mass growth rate in addition to tree mass, the resulting model fits were generally linear, as predicted by metabolic scaling theory[6] (Extended Data Fig. 2). Similar to the results of our main

[1]US Geological Survey, Western Ecological Research Center, Three Rivers, California 93271, USA. [2]Smithsonian Tropical Research Institute, Apartado 0843-03092, Balboa, Republic of Panama. [3]School of Biological Sciences, University of Nebraska, Lincoln, Nebraska 68588, USA. [4]Department of Forest and Ecosystem Science, University of Melbourne, Victoria 3121, Australia. [5]Department of Plant Sciences, University of Cambridge, Cambridge CB2 3EA, UK. [6]Department of Geography, University College London, London WC1E 6BT, UK. [7]School of Botany, University of Melbourne, Victoria 3010, Australia. [8]Spezielle Botanik und Funktionelle Biodiversität, Universität Leipzig, 04103 Leipzig, Germany. [9]Jardín Botánico de Medellín, Calle 73, No. 51D-14, Medellín, Colombia. [10]Instituto de Ecología Regional, Universidad Nacional de Tucumán, 4107 Yerba Buena, Tucumán, Argentina. [11]Research Office, Department of National Parks, Wildlife and Plant Conservation, Bangkok 10900, Thailand. [12]Department of Botany and Plant Physiology, Buea, Southwest Province, Cameroon. [13]Smithsonian Institution Global Earth Observatory—Center for Tropical Forest Science, Smithsonian Institution, PO Box 37012, Washington, DC 20013, USA. [14]Universidad Nacional de Colombia, Departamento de Ciencias Forestales, Medellín, Colombia. [15]Wildlife Conservation Society, Kinshasa/Gombe, Democratic Republic of the Congo. [16]Unité Mixte de Recherche—Peuplements Végétaux et Bioagresseurs en Milieu Tropical, Université de la Réunion/CIRAD, 97410 Saint Pierre, France. [17]School of Environmental and Forest Sciences, University of Washington, Seattle, Washington 98195, USA. [18]State Key Laboratory of Forest and Soil Ecology, Institute of Applied Ecology, Chinese Academy of Sciences, Shenyang 110164, China. [19]Department of Forest Ecosystems and Society, Oregon State University, Corvallis, Oregon 97331, USA. [20]Department of Ecology and Evolutionary Biology, University of California, Los Angeles, California 90095, USA. [21]Department of Life Science, Tunghai University, Taichung City 40704, Taiwan. [22]Facultad de Ciencias Agrarias, Universidad Nacional de Jujuy, 4600 San Salvador de Jujuy, Argentina. [23]Faculty of Forestry, Kasetsart University, ChatuChak Bangkok 10900, Thailand. [24]Taiwan Forestry Research Institute, Taipei 10066, Taiwan. [25]Department of Natural Resources and Environmental Studies, National Dong Hwa University, Hualien 97401, Taiwan. [26]Sarawak Forestry Department, Kuching, Sarawak 93660, Malaysia. [27]Department of Botany and Plant Pathology, Oregon State University, Corvallis, Oregon 97331, USA. [28]US Geological Survey, Western Ecological Research Center, Arcata, California 95521, USA. [29]Landcare Research, PO Box 40, Lincoln 7640, New Zealand. [30]Forest Ecology and Restoration Group, Department of Life Sciences, University of Alcalá, Alcalá de Henares, 28805 Madrid, Spain. †Present addresses: Mathematical Biosciences Institute, Ohio State University, Columbus, Ohio 43210, USA (N.G.B.); German Centre for Integrative Biodiversity Research (iDiv), Halle-Jena-Leipzig, 04103 Leipzig, Germany (N.R.).

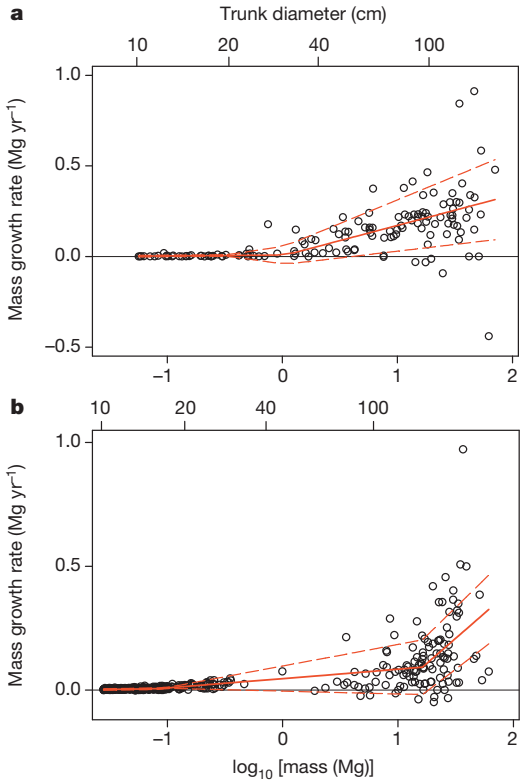

Figure 1 | Example model fits for tree mass growth rates. The species shown are the angiosperm species (*Lecomtedoxa klaineana*, Cameroon, 142 trees) (**a**) and gymnosperm species (*Picea sitchensis*, USA, 409 trees) (**b**) in our data set that had the most massive trees (defined as those with the greatest cumulative aboveground dry mass in their five most massive trees). Each point represents a single tree; the solid red lines represent best fits selected by our model; and the dashed red lines indicate one standard deviation around the predicted values.

analysis using untransformed growth, of the 381 log-transformed species analysed (see Methods), the log-transformed growth rate increased in the bin containing the largest trees for 96% of species.

In absolute terms, trees 100 cm in trunk diameter typically add from 10 kg to 200 kg of aboveground dry mass each year (depending on species), averaging 103 kg per year. This is nearly three times the rate for trees of the same species at 50 cm in diameter, and is the mass equivalent to adding an entirely new tree of 10–20 cm in diameter to the forest each year. Our findings further indicate that the extraordinary growth recently reported in an intensive study of large *Eucalyptus regnans* and *Sequoia sempervirens*[7], which included some of the world's most massive individual trees, is not a phenomenon limited to a few unusual species. Rather, rapid growth in giant trees is the global norm, and can exceed 600 kg per year in the largest individuals (Fig. 3).

Our data set included many natural and unmanaged forests in which the growth of smaller trees was probably reduced by asymmetric competition with larger trees. To explore the effects of competition, we calculated mass growth rates for 41 North American and European species that had published equations for diameter growth rate in the absence of competition. We found that, even in the absence of competition, 85% of the species had mass growth rates that increased continuously with tree size (Extended Data Fig. 3), with growth curves closely resembling those in Fig. 2. Thus, our finding of increasing growth not only has broad generality across species, continents and forest biomes (tropical, subtropical and temperate), it appears to hold regardless of competitive environment.

Importantly, our finding of continuously increasing growth is compatible with the two classes of observations most often cited as evidence of declining, rather than increasing, individual tree growth: with increasing tree size and age, productivity usually declines at the scales of both tree organs (leaves) and tree populations (even-aged forest stands).

First, although growth efficiency (tree mass growth per unit leaf area or leaf mass) often declines with increasing tree size[8–10], empirical observations and metabolic scaling theory both indicate that, on average, total tree leaf mass increases as the square of trunk diameter[17,18]. A typical tree that experiences a tenfold increase in diameter will therefore undergo a roughly 100-fold increase in total leaf mass and a 50–100-fold

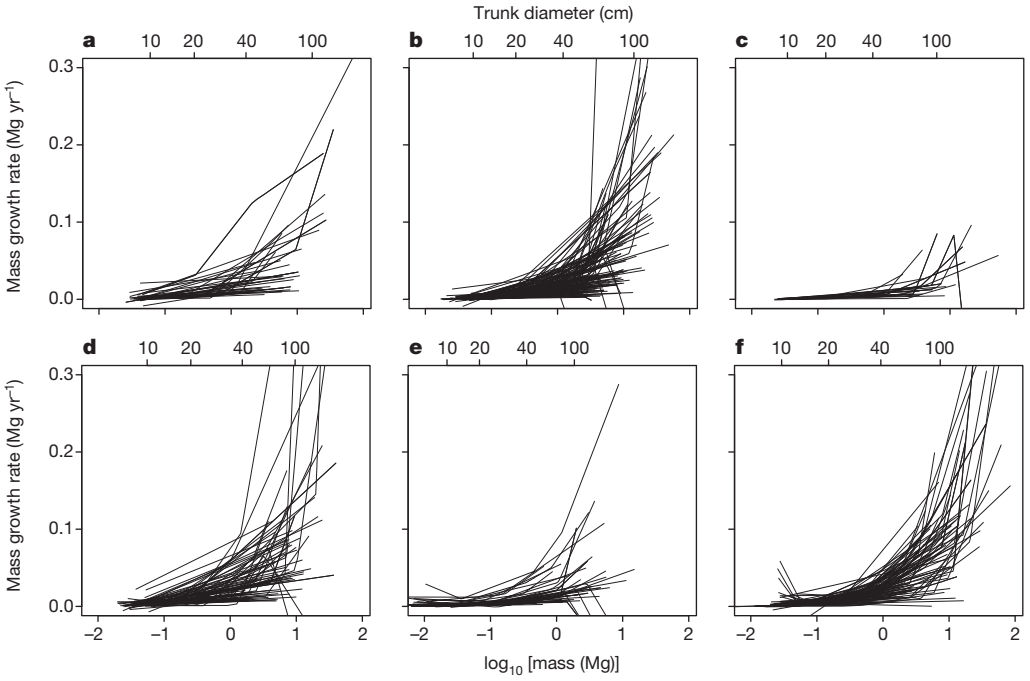

Figure 2 | Aboveground mass growth rates for the 403 tree species, by continent. **a**, Africa (Cameroon, Democratic Republic of the Congo); **b**, Asia (China, Malaysia, Taiwan, Thailand); **c**, Australasia (New Zealand); **d**, Central and South America (Argentina, Colombia, Panama); **e**, Europe (Spain); and **f**, North America (USA). Numbers of trees, numbers of species and percentages with increasing growth are given in Table 1. Trunk diameters are approximate values for reference, based on the average diameters of trees of a given mass.

Table 1 | Sample sizes and tree growth trends by continent

Continent	Number of trees	Number of species	Percentage of species with increasing mass growth rate in the largest trees (percentage significant at $P \leq 0.05$)
Africa	15,366	37	100.0 (86.5)
Asia	43,690	136	96.3 (89.0)
Australasia	45,418	22	95.5 (95.5)
Central and South America	18,530	77	97.4 (92.2)
Europe	439,889	42	90.5 (78.6)
North America	110,153	89	98.9 (94.4)
Total	673,046	403	96.8 (89.8)

The largest trees are those in the last bin fitted by the model. Countries are listed in the legend for Fig. 2.

increase in total leaf area (depending on size-related increases in leaf mass per unit leaf area[19,20]). Parallel changes in growth efficiency can range from a modest increase (such as in stands where small trees are suppressed by large trees)[21] to as much as a tenfold decline[22], with most changes falling in between[8,9,19,22]. At one extreme, the net effect of a low (50-fold) increase in leaf area combined with a large (tenfold) decline in growth efficiency would still yield a fivefold increase in individual tree mass growth rate; the opposite extreme would yield roughly a 100-fold increase. Our calculated 52-fold greater average mass growth rate of trees 100 cm in diameter compared to those 10 cm in diameter falls within this range. Thus, although growth efficiency often declines with increasing tree size, increases in a tree's total leaf area are sufficient to overcome this decline and cause whole-tree carbon accumulation rate to increase.

Second, our findings are similarly compatible with the well-known age-related decline in productivity at the scale of even-aged forest stands. Although a review of mechanisms is beyond the scope of this paper[10,23], several factors (including the interplay of changing growth efficiency and tree dominance hierarchies[24]) can contribute to declining productivity at the stand scale. We highlight the fact that increasing individual tree growth rate does not automatically result in increasing stand productivity because tree mortality can drive orders-of-magnitude reductions in population density[25,26]. That is, even though the large trees in older, even-aged stands may be growing more rapidly, such stands have fewer trees. Tree population dynamics, especially mortality, can thus be a significant contributor to declining productivity at the scale of the forest stand[23].

For a large majority of species, our findings support metabolic scaling theory's qualitative prediction of continuously increasing growth at the scale of individual trees[6], with several implications. For example, life-history theory often assumes that tradeoffs between plant growth and reproduction are substantial[11]. Contrary to some expectations[11,16], our results indicate that for most tree species size-related changes in reproductive allocation are insufficient to drive long-term declines in growth rates[6]. Additionally, declining growth is sometimes considered to be a defining feature of plant senescence[12]. Our findings are thus relevant to understanding the nature and prevalence of senescence in the life history of perennial plants[27].

Finally, our results are relevant to understanding and predicting forest feedbacks to the terrestrial carbon cycle and global climate system[1–3]. These feedbacks will be influenced by the effects of climatic, land-use and other environmental changes on the size-specific growth rates and size structure of tree populations—effects that are already being observed in forests[28,29]. The rapid growth of large trees indicates that, relative to their numbers, they could play a disproportionately important role in these feedbacks[30]. For example, in our western USA old-growth forest plots, trees >100 cm in diameter comprised 6% of trees, yet contributed 33% of the annual forest mass growth. Mechanistic models of the forest carbon cycle will depend on accurate representation of productivity across several scales of biological organization, including calibration and validation against continuously increasing carbon accumulation rates at the scale of individual trees.

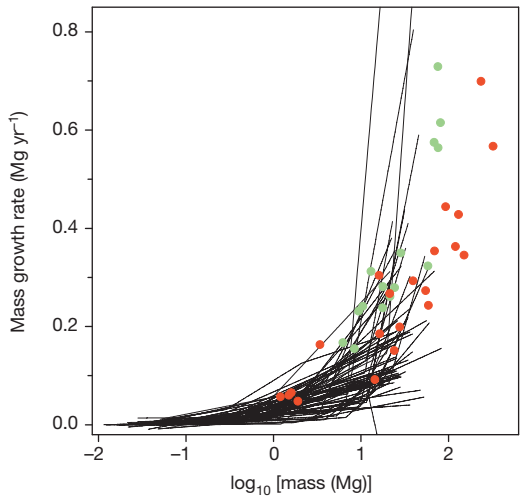

Figure 3 | Aboveground mass growth rates of species in our data set compared with *E. regnans* and *S. sempervirens*. For clarity, only the 58 species in our data set having at least one tree exceeding 20 Mg are shown (lines). Data for *E. regnans* (green dots, 15 trees) and *S. sempervirens* (red dots, 21 trees) are from an intensive study that included some of the most massive individual trees on Earth[7]. Both axes are expanded relative to those of Fig. 2.

METHODS SUMMARY

We estimated aboveground dry mass growth rates from consecutive diameter measurements of tree trunks—typically measured every five to ten years—from long-term monitoring plots. Analyses were restricted to trees with trunk diameter ≥10 cm, and to species having ≥40 trees in total and ≥15 trees with trunk diameter ≥30 cm. Maximum trunk diameters ranged from 38 cm to 270 cm among species, averaging 92 cm. We converted each diameter measurement (plus an accompanying height measurement for 16% of species) to aboveground dry mass, M, using published allometric equations. We estimated tree growth rate as $G = \Delta M/\Delta t$ and modelled G as a function of $\log(M)$ for each species using piecewise regression. The independent variable $\log(M)$ was divided into bins and a separate line segment was fitted to G versus $\log(M)$ in each bin so that the line segments met at the bin divisions. Bin divisions were not assigned a priori, but were fitted by the model separately for each species. We fitted models with 1, 2, 3 and 4 bins, and selected the model receiving the most support by Akaike's Information Criterion for each species. Our approach thus makes no assumptions about the shape of the relationship between G and $\log(M)$, and can accommodate increasing, decreasing or hump-shaped relationships. Parameters were fitted with a Gibbs sampler based on Metropolis updates, producing credible intervals for model parameters and growth rates at any diameter; uninformative priors were used for all parameters. We tested extensively for bias, and found no evidence that our results were influenced by model fits failing to detect a final growth decline in the largest trees, possible biases introduced by the 47% of species for which we combined data from several plots, or possible biases introduced by allometric equations (Extended Data Figs 4 and 5).

Online Content Any additional Methods, Extended Data display items and Source Data are available in the online version of the paper; references unique to these sections appear only in the online paper.

Received 5 August; accepted 27 November 2013.
Published online 15 January 2014.

1. Pan, Y. *et al.* A large and persistent carbon sink in the world's forests. *Science* **333,** 988–993 (2011).

2. Medvigy, D., Wofsy, S. C., Munger, J. W., Hollinger, D. Y. & Moorcroft, P. R. Mechanistic scaling of ecosystem function and dynamics in space and time: Ecosystem Demography model version 2. *J. Geophys. Res.* **114,** G01002 (2009).
3. Caspersen, J. P., Vanderwel, M. C., Cole, W. G. & Purves, D. W. How stand productivity results from size- and competition-dependent growth and mortality. *PLoS ONE* **6,** e28660 (2011).
4. Kutsch, W. L. *et al.* in *Old-Growth Forests: Function, Fate and Value* (eds Wirth, C., Gleixner, G. & Heimann, M.) 57–79 (Springer, 2009).
5. Meinzer, F. C., Lachenbruch, B. & Dawson, T. E. (eds) *Size- and Age-Related Changes in Tree Structure and Function* (Springer, 2011).
6. Enquist, B. J., West, G. B., Charnov, E. L. & Brown, J. H. Allometric scaling of production and life-history variation in vascular plants. *Nature* **401,** 907–911 (1999).
7. Sillett, S. C. *et al.* Increasing wood production through old age in tall trees. *For. Ecol. Manage.* **259,** 976–994 (2010).
8. Mencuccini, M. *et al.* Size-mediated ageing reduces vigour in trees. *Ecol. Lett.* **8,** 1183–1190 (2005).
9. Drake, J. E., Raetz, L. M., Davis, S. C. & DeLucia, E. H. Hydraulic limitation not declining nitrogen availability causes the age-related photosynthetic decline in loblolly pine (*Pinus taeda* L.). *Plant Cell Environ.* **33,** 1756–1766 (2010).
10. Ryan, M. G., Binkley, D. & Fownes, J. H. Age-related decline in forest productivity: pattern and process. *Adv. Ecol. Res.* **27,** 213–262 (1997).
11. Thomas, S. C. in *Size- and Age-Related Changes in Tree Structure and Function* (eds Meinzer, F. C., Lachenbruch, B. & Dawson, T. E.) 33–64 (Springer, 2011).
12. Thomas, H. Senescence, ageing and death of the whole plant. *New Phytol.* **197,** 696–711 (2013).
13. Carey, E. V., Sala, A., Keane, R. & Callaway, R. M. Are old forests underestimated as global carbon sinks? *Glob. Change Biol.* **7,** 339–344 (2001).
14. Phillips, N. G., Buckley, T. N. & Tissue, D. T. Capacity of old trees to respond to environmental change. *J. Integr. Plant Biol.* **50,** 1355–1364 (2008).
15. Piper, F. I. & Fajardo, A. No evidence of carbon limitation with tree age and height in *Nothofagus pumilio* under Mediterranean and temperate climate conditions. *Ann. Bot.* **108,** 907–917 (2011).
16. Weiner, J. & Thomas, S. C. The nature of tree growth and the ''age-related decline in forest productivity''. *Oikos* **94,** 374–376 (2001).
17. Jenkins, J. C., Chojnacky, D. C., Heath, L. S. & Birdsey, R. A. *Comprehensive Database of Diameter-based Biomass Regressions for North American Tree Species* General Technical Report NE-319, http://www.nrs.fs.fed.us/pubs/6725 (USDA Forest Service, Northeastern Research Station, 2004).
18. Niklas, K. J. & Enquist, B. J. Canonical rules for plant organ biomass partitioning and annual allocation. *Am. J. Bot.* **89,** 812–819 (2002).
19. Thomas, S. C. Photosynthetic capacity peaks at intermediate size in temperate deciduous trees. *Tree Physiol.* **30,** 555–573 (2010).
20. Steppe, K., Niinemets, Ü. & Teskey, R. O. in *Size- and Age-Related Changes in Tree Structure and Function* (eds Meinzer, F. C., Lachenbruch, B. & Dawson, T. E.) 235–253 (Springer, 2011).
21. Gilmore, D. W. & Seymour, R. S. Alternative measures of stem growth efficiency applied to *Abies balsamea* from four canopy positions in central Maine, USA. *For. Ecol. Manage.* **84,** 209–218 (1996).
22. Kaufmann, M. R. & Ryan, M. G. Physiographic, stand, and environmental effects on individual tree growth and growth efficiency in subalpine forests. *Tree Physiol.* **2,** 47–59 (1986).
23. Coomes, D. A., Holdaway, R. J., Kobe, R. K., Lines, E. R. & Allen, R. B. A general integrative framework for modelling woody biomass production and carbon sequestration rates in forests. *J. Ecol.* **100,** 42–64 (2012).
24. Binkley, D. A hypothesis about the interaction of tree dominance and stand production through stand development. *For. Ecol. Manage.* **190,** 265–271 (2004).
25. Pretzsch, H. & Biber, P. A re-evaluation of Reineke's rule and stand density index. *For. Sci.* **51,** 304–320 (2005).
26. Kashian, D. M., Turner, M. G., Romme, W. H. & Lorimer, C. G. Variability and convergence in stand structural development on a fire-dominated subalpine landscape. *Ecology* **86,** 643–654 (2005).
27. Munné-Bosch, S. Do perennials really senesce? *Trends Plant Sci.* **13,** 216–220 (2008).
28. Jump, A. S., Hunt, J. M. & Peñuelas, J. Rapid climate change-related growth decline at the southern range edge of *Fagus sylvatica. Glob. Change Biol.* **12,** 2163–2174 (2006).
29. Lindenmayer, D. B., Laurance, W. F. & Franklin, J. F. Global decline in large old trees. *Science* **338,** 1305–1306 (2012).
30. Enquist, B. J., West, G. B. & Brown, J. H. Extensions and evaluations of a general quantitative theory of forest structure and dynamics. *Proc. Natl Acad. Sci. USA* **106,** 7046–7051 (2009).

Supplementary Information is available in the online version of the paper.

Acknowledgements We thank the hundreds of people who have established and maintained the forest plots and their associated databases; M. G. Ryan for comments on the manuscript; C. D. Canham and T. Hart for supplying data; C. D. Canham for discussions and feedback; J. S. Baron for hosting our workshops; and Spain's Ministerio de Agricultura, Alimentación y Medio Ambiente (MAGRAMA) for granting access to the Spanish Forest Inventory Data. Our analyses were supported by the United States Geological Survey (USGS) John Wesley Powell Center for Analysis and Synthesis, the USGS Ecosystems and Climate and Land Use Change mission areas, the Smithsonian Institution Global Earth Observatory—Center for Tropical Forest Science (CTFS), and a University of Nebraska-Lincoln Program of Excellence in Population Biology Postdoctoral Fellowship (to N.G.B.). In addition, X.W. was supported by National Natural Science Foundation of China (31370444) and State Key Laboratory of Forest and Soil Ecology (LFSE2013-11). Data collection was funded by a broad range of organizations including the USGS, the CTFS, the US National Science Foundation, the Andrews LTER (NSF-LTER DEB-0823380), the US National Park Service, the US Forest Service (USFS), the USFS Forest Inventory and Analysis Program, the John D. and Catherine T. MacArthur Foundation, the Andrew W. Mellon Foundation, MAGRAMA, the Council of Agriculture of Taiwan, the National Science Council of Taiwan, the National Natural Science Foundation of China, the Knowledge Innovation Program of the Chinese Academy of Sciences, Landcare Research and the National Vegetation Survey Database (NVS) of New Zealand, the French Fund for the Global Environment and Fundación ProYungas. This paper is a contribution from the Western Mountain Initiative, a USGS global change research project. Any use of trade names is for descriptive purposes only and does not imply endorsement by the USA government.

Author Contributions N.L.S. and A.J.D. conceived the study with feedback from R.C. and D.A.C., N.L.S., A.J.D., R.C. and S.E.R. wrote the manuscript. R.C. devised the main analytical approach and wrote the computer code. N.L.S., A.J.D., R.C., S.E.R., P.J.B., N.G.B., D.A.C., E.R.L., W.K.M. and N.R. performed analyses. N.L.S., A.J.D., R.C., S.E.R., P.J.B., D.A.C., E.R.L., W.K.M., E.Á., C.B., S.B., G.C., S.J.D., Á.D., C.N.E., O.F., J.F.F., H.R.G., Z.H., M.E.H., S.P.H., D.K., Y.L., J.-R.M., A.M., L.R.M., R.J.P., N.P., S.-H.S., I-F.S., S.T., D.T., P.J.v.M., X.W., S.K.W. and M.A.Z. supplied data and sources of allometric equations appropriate to their data.

Author Information Fitted model parameters for each species have been deposited in USGS's ScienceBase at http://dx.doi.org/10.5066/F7JS9NFM. Reprints and permissions information is available at www.nature.com/reprints. The authors declare no competing financial interests. Readers are welcome to comment on the online version of the paper. Correspondence and requests for materials should be addressed to N.L.S. (nstephenson@usgs.gov).

METHODS

Data. We required that forest monitoring plots provided unbiased samples of all living trees within the plot boundaries, and that the trees had undergone two trunk diameter measurements separated by at least one year. Some plots sampled minimally disturbed old (all-aged) forest, whereas others, particularly those associated with national inventories, sampled forest stands regardless of past management history. Plots are described in the references cited in Supplementary Table 1.

Our raw data were consecutive measurements of trunk diameter, D, with most measurements taken 5 to 10 years apart (range, 1–29 years). D was measured at a standard height on the trunk (usually 1.3–1.4 m above ground level), consistent across measurements for a tree. Allometric equations for 16% of species required, in addition to consecutive measurements of D, consecutive measurements of tree height.

We excluded trees exhibiting extreme diameter growth, defined as trunks where D increased by $\geq 40\ \mathrm{mm\ yr^{-1}}$ or that shrank by $\geq 12s$, where s is the standard deviation of the D measurement error, $s = 0.9036 + 0.006214D$ (refs 31, 32); outliers of these magnitudes were almost certainly due to error. By being so liberal in allowing negative growth anomalies, we erred on the side of reducing our ability to detect increases in tree mass growth rate. Using other exclusion values yielded similar results, as did a second approach to handling error in which we reanalysed a subset of our models using a Bayesian method that estimates growth rates after accounting for error, based on independent plot-specific data quantifying measurement error[33].

To standardize minimum D among data sets, we analysed only trees with $D \geq 10$ cm at the first census. To ensure adequate samples of trees spanning a broad range of sizes, we restricted analyses to species having both ≥ 40 trees in total and also ≥ 15 trees with $D \geq 30$ cm at the first census. This left us with 673,046 trees belonging to 403 tropical and temperate species in 76 families, spanning twelve countries and all forested continents (Supplementary Table 1). Maximum trunk diameters ranged from 38 cm to 270 cm among species, and averaged 92 cm.

Estimating tree mass. To estimate each tree's aboveground dry mass, M, we used published allometric equations relating M to D (or for 16% of species, relating M to D and tree height). Some equations were species-specific and others were specific to higher taxonomic levels or forest types, described in the references in Supplementary Table 1. The single tropical moist forest equation of ref. 34 was applied to most tropical species, whereas most temperate species had unique species-specific equations. Most allometric equations are broadly similar, relating $\log(M)$ to $\log(D)$ linearly, or nearly linearly—a familiar relationship in allometric scaling of both animals and plants[35]. Equations can show a variety of differences in detail, however, with some adding $\log(D)$ squared and cubed terms. All equations make use of the wood density of individual species, but when wood density was not available for a given species we used mean wood density for a genus or family[36].

Using a single, average allometry for most tropical species, and mean wood density for a genus or family for several species, limits the accuracy of our estimates of M. However, because we treat each species separately, it makes no difference whether our absolute M estimates are more accurate in some species than in others, only that they are consistent within a species and therefore accurately reveal whether mass growth rates increase or decrease with tree size.

For two regions—Spain and the western USA—allometric equations estimated mass only for a tree's main stem rather than all aboveground parts, including branches and leaves. But because leaf and stem masses are positively correlated and their growth rates are expected to scale isometrically both within and among species[18,37,38], results from these two regions should not alter our qualitative conclusions. Confirming this, the percentage of species with increasing stem mass growth rate in the last bin for Spain and the western USA (93.4% of 61 species) was similar to that from the remainder of regions (97.4% of 342 species) ($P = 0.12$, Fisher's exact test).

Modelling mass growth rate. We sought a modelling approach that made no assumptions about the shape of the relationship between aboveground dry mass growth rate, G, and aboveground dry mass, M, and that could accommodate monotonically increasing, monotonically decreasing, or hump-shaped relationships. We therefore chose to model G as a function of $\log(M)$ using piecewise linear regression. The range of the x axis, $X = \log(M)$, is divided into a series of bins, and within each bin G is fitted as a function of X by linear regression. The position of the bins is adaptive: it is fitted along with the regression terms. Regression lines are required to meet at the boundary between bins. For a single model-fitting run the number of bins, B, is fixed. For example, if $B = 2$, there are four parameters to be fitted for a single species: the location of the boundary between bins, X_1; the slope of the regression in the first bin, S_1; the slope in the second bin, S_2; and an intercept term. Those four parameters completely define the model. In general, there are $2B$ parameters for B bins.

Growth rates, while approximately normally distributed, were heteroskedastic, with the variance increasing with mass (Fig. 1), so an additional model was needed for the standard deviation of G, σ_G, as a function of $\log(M)$. The increase of σ_G with $\log(M)$ was clearly not linear, so we used a three-parameter model:

$$\sigma_G = k \qquad (\text{for } \log(M) < d)$$

$$\sigma_G = a + b\log(M) \qquad (\text{for } \log(M) \geq d)$$

where the intercept a is determined by the values of k, d and b. Thus σ_G was constant for smaller values of $\log(M)$ (below the cutoff d), then increased linearly for larger $\log(M)$ (Fig. 1). The parameters k, d and b were estimated along with the parameters of the growth model.

Parameters of both the growth and standard deviation models were estimated in a Bayesian framework using the likelihood of observing growth rates given model predictions and the estimated standard deviation of the Gaussian error function. A Markov chain Monte Carlo chain of parameter estimates was created using a Gibbs sampler with a Metropolis update[39,40] written in the programming language R (ref. 41) (a tutorial and the computer code are available through http://ctfs.arnarb.harvard.edu/Public/CTFSRPackage/files/tutorials/growthfitAnalysis). The sampler works by updating each of the parameters in sequence, holding other parameters fixed while the relevant likelihood function is used to locate the target parameter's next value. The step size used in the updates was adjusted adaptively through the runs, allowing more rapid convergence[40]. The final Markov chain Monte Carlo chain describes the posterior distribution for each model parameter, the error, and was then used to estimate the posterior distribution of growth rates as estimated from the model. Priors on model parameters were uniform over an unlimited range, whereas the parameters describing the standard deviation were restricted to >0. Bin boundaries, X_i, were constrained as follows: (1) boundaries could only fall within the range of X, (2) each bin contained at least five trees, and (3) no bin spanned less than 10% of the range of X. The last two restrictions prevented the bins from collapsing to very narrow ranges of X in which the fitted slope might take absurd extremes.

We chose piecewise regression over other alternatives for modelling G as a function of M for two main reasons. First, the linear regression slopes within each bin provide precise statistical tests of whether G increases or decreases with X, based on credible intervals of the slope parameters. Second, with adaptive bin positions, the function is completely flexible in allowing changes in slope at any point in the X range, with no influence of any one bin on the others. In contrast, in parametric models where a single function defines the relationship across all X, the shape of the curve at low X can (and indeed must) influence the shape at high X, hindering statistical inference about changes in tree growth at large size.

We used $\log(M)$ as our predictor because within a species M has a highly non-Gaussian distribution, with many small trees and only a few very large trees, including some large outliers. In contrast, we did not log-transform our dependent variable G so that we could retain values of $G \leq 0$ that are often recorded in very slowly growing trees, for which diameter change over a short measurement interval can be on a par with diameter measurement error.

For each species, models with 1, 2, 3 and 4 bins were fitted. Of these four models, the model receiving the greatest weight of evidence by Akaike Information Criterion (AIC) was selected. AIC is defined as the log-likelihood of the best-fitting model, penalized by twice the number of parameters. Given that adding one more bin to a model meant two more parameters, the model with an extra bin had to improve the log-likelihood by 4 to be considered a better model[42].

Assessing model fits. To determine whether our approach might have failed to reveal a final growth decline within the few largest trees of the various species, we calculated mass growth rate residuals for the single most massive individual tree of each species. For 52% of the 403 species, growth of the most massive tree was underestimated by our model fits (for example, Fig. 1a); for 48% it was overestimated (for example, Fig. 1b). These proportions were indistinguishable from 50% ($P = 0.55$, binomial test), as would be expected for unbiased model fits. Furthermore, the mean residual (observed minus predicted) mass growth rate of these most massive trees, $+0.006\ \mathrm{Mg\ yr^{-1}}$, was statistically indistinguishable from zero ($P = 0.29$, two-tailed t-test). We conclude that our model fits accurately represent growth trends up through, and including, the most massive trees.

Effects of combined data. To achieve sample sizes adequate for analysis, for some species we combined data from several different forest plots, potentially introducing a source of bias: if the largest trees of a species disproportionately occur on productive sites, the increase in mass growth rate with tree size could be exaggerated. This might occur because trees on less-productive sites—presumably the sites having the slowest-growing trees within any given size class—could be underrepresented in the largest size classes. We assessed this possibility in two ways.

First, our conclusions remained unchanged when we compared results for the 53% of species that came uniquely from single large plots with those of the 47% of species whose data were combined across several plots. Proportions of species with increasing mass growth rates in the last bin were indistinguishable between the two groups (97.6% and 95.8%, respectively; $P = 0.40$, Fisher's exact test). Additionally,

the shapes and magnitudes of the growth curves for Africa and Asia, where data for each species came uniquely from single large plots, were similar to those of Australasia, Europe and North America, where data for each species were combined across several plots (Table 1, Fig. 2 and Extended Data Fig. 2). (Data from Central and South America were from both single and combined plots, depending on species.)

Second, for a subset of combined-data species we compared two sets of model fits: (1) using all available plots (that is, the analyses we present in the main text), and (2) using only plots that contained massive trees—those in the top 5% of mass for a species. To maximize our ability to detect differences, we limited these analyses to species with large numbers of trees found in a large number of plots, dispersed widely across a broad geographic region. We therefore analysed the twelve Spanish species that each had more than 10,000 individual trees (Supplementary Table 1), found in 34,580 plots distributed across Spain. Massive trees occurred in 6,588 (19%) of the 34,580 plots. We found no substantial differences between the two analyses. When all 34,580 plots were analysed, ten of the twelve species showed increasing growth in the last bin, and seven showed increasing growth across all bins; when only the 6,588 plots containing the most massive trees were analysed, the corresponding numbers were eleven and nine. Model fits for the two groups were nearly indistinguishable in shape and magnitude across the range of tree masses. We thus found no evidence that the potential for growth differences among plots influenced our conclusions.

Effects of possible allometric biases. For some species, the maximum trunk diameter D in our data sets exceeded the maximum used to calibrate the species' allometric equation. In such cases our estimates of M extrapolate beyond the fitted allometry and could therefore be subject to bias. For 336 of our 403 species we were able to determine D of the largest tree that had been used in calibrating the associated allometric equations. Of those 336 species, 74% (dominated by tropical species) had no trees in our data set with D exceeding that used in calibrating the allometric equations, with the remaining 26% (dominated by temperate species) having at least one tree with D exceeding that used in calibration. The percentage of species with increasing G in the last bin for the first group (98.0%) was indistinguishable from that of the second group (96.6%) ($P = 0.44$, Fisher's exact test). Thus, our finding of increasing G with tree size is not affected by the minority of species that have at least one tree exceeding the maximum value of D used to calibrate their associated allometric equations.

A bias that could inflate the rate at which G increases with tree size could arise if allometric equations systematically underestimate M for small trees or overestimate M for large trees[43]. For a subset of our study species we obtained the raw data—consisting of measured values of D and M for individual trees—needed to calibrate allometric equations, allowing us to determine whether the particular form of those species' allometric equations was prone to bias, and if so, the potential consequences of that bias.

To assess the potential for allometric bias for the majority (58%) of species in our data set—those that used the empirical moist tropical forest equation of ref. 34—we reanalysed the data provided by ref. 34. The data were from 1,504 harvested trees representing 60 families and 184 genera, with D ranging from 5 cm to 156 cm; the associated allometric equation relates $\log(M)$ to a third-order polynomial of $\log(D)$. Because the regression of M on D was fitted on a log–log scale, this and subsequent equations include a correction of $\exp[(\mathrm{RSE})^2/2]$ for the error in back-transformation, where RSE is the residual standard error from the statistical model[44]. Residuals of M for the equation revealed no evident biases (Extended Data Fig. 4a), suggesting that we should expect little (if any) systematic size-related biases in our estimates of G for the 58% of our species that used this equation.

Our simplest form of allometric equation—applied to 22% of our species—was $\log(M) = a + b\log(D)$, where a and b are taxon-specific constants. For nine of our species that used equations of this form (all from the temperate western USA: *Abies amabilis, A. concolor, A. procera, Pinus lambertiana, Pinus ponderosa, Picea sitchensis, Pseudotsuga menziesii, Tsuga heterophylla* and *T. mertensiana*) we had values of both D and M for a total of 1,358 individual trees, allowing us to fit species-specific allometric equations of the form $\log(M) = a + b\log(D)$ and then assess them for bias. Residual plots showed a tendency to overestimate M for the largest trees (Extended Data Fig. 4b), with the possible consequence of inflating estimates of G for the largest relative to the smallest trees of these species.

To determine whether this bias was likely to alter our qualitative conclusion that G increases with tree size, we created a new set of allometric relations between D and M —one for each of the nine species—using the same piecewise linear regression approach we used to model G as a function of M. However, because our goal was to eliminate bias rather than seek the most parsimonious model, we fixed the number of bins at four, with the locations of boundaries between the bins being fitted by the model. Our new allometry using piecewise regressions led to predictions of M with no apparent bias relative to D (Extended Data Fig. 4c). This new, unbiased allometry gave the same qualitative results as our original, simple allometry regarding the relationship between G and M: for all nine species, G increased in the bin containing the largest trees, regardless of the allometry used (Extended Data Fig. 5). We conclude that any bias associated with the minority of our species that used the simple allometric equation form was unlikely to affect our broad conclusion that G increases with tree size in a majority of tree species.

As a final assessment, we compared our results to those of a recent study of *E. regnans* and *S. sempervirens*, in which M and G had been calculated from intensive measurements of aboveground portions of trees without the use of standard allometric equations[7]. Specifically, in two consecutive years 36 trees of different sizes and ages were climbed, trunk diameters were systematically measured at several heights, branch diameters and lengths were measured (with subsets of foliage and branches destructively sampled to determine mass relationships), wood densities were determined and ring widths from increment cores were used to supplement measured diameter growth increments. The authors used these measurements to calculate M for each of the trees in each of the two consecutive years, and G as the difference in M between the two years[7]. *E. regnans* and *S. sempervirens* are the world's tallest angiosperm and gymnosperm species, respectively, so the data set was dominated by exceptionally large trees; most had $M \geq 20$ Mg, and M of some individuals exceeded that of the most massive trees in our own data set (which lacked *E. regnans* and *S. sempervirens*). We therefore compared *E. regnans* and *S. sempervirens* to the 58 species in our data set that had at least one individual with $M \geq 20$ Mg. Sample sizes for *E. regnans* and *S. sempervirens*—15 and 21 trees, respectively—fell below our required ≥40 trees for fitting piecewise linear regressions, so we simply plotted data points for individual *E. regnans* and *S. sempervirens* along with the piecewise regressions that we had already fitted for our 58 comparison species (Fig. 3).

As reported by ref. 7, G increased with M for both *E. regnans* and *S. sempervirens*, up to and including some of the most massive individual trees on the Earth (Fig. 3). Within the zone of overlapping M between the two data sets, G values for individual *E. regnans* and *S. sempervirens* trees fell almost entirely within the ranges of the piecewise regressions we had fitted for our 58 comparison species. We take these observations as a further indication that our results, produced using standard allometric equations, accurately reflect broad relationships between M and G.

Fitting log–log models. To model $\log(G)$ as a function of $\log(M)$, we used the binning approach that we used in our primary analysis of mass growth rate (described earlier). However, in log-transforming growth we dropped trees with $G \leq 0$. Because negative growth rates become more extreme with increasing tree size, dropping them could introduce a bias towards increasing growth rates. Log-transformation additionally resulted in skewed growth rate residuals. Dropping trees with $G \leq 0$ caused several species to fall below our threshold sample size, reducing the total number of species analysed to 381 (Extended Data Fig. 2).

Growth in the absence of competition. We obtained published equations for 41 North American and European species, in 46 species-site combinations, relating species-specific tree diameter growth rates to trunk diameter D and to neighbourhood competition[45–49]. Setting neighbourhood competition to zero gave us equations describing estimated annual D growth as a function of D in the absence of competition. Starting at $D_0 = 10$ cm, we sequentially (1) calculated annual D growth for a tree of size D_t, (2) added this amount to D_t to determine D_{t+1}, (3) used an appropriate taxon-specific allometric equation to calculate the associated tree masses M_t and M_{t+1}, and (iv) calculated tree mass growth rate G_t of a tree of mass M_t in the absence of competition as $M_{t+1} - M_t$. For each of the five species that had separate growth analyses available from two different sites, we required that mass growth rate increased continuously with tree size at both sites for the species to be considered to have a continuously increasing mass growth rate. North American and European allometries were taken from refs 17 and 50, respectively, with preference given to allometric equations based on power functions of tree diameter, large numbers of sampled trees, and trees spanning a broad range of diameters. For the 47% of European species for which ref. 50 had no equations meeting our criteria, we used the best-matched (by species or genus) equations from ref. 17.

31. Condit, R. *et al.* Tropical forest dynamics across a rainfall gradient and the impact of an El Niño dry season. *J. Trop. Ecol.* **20,** 51–72 (2004).
32. Condit, R. *et al.* The importance of demographic niches to tree diversity. *Science* **313,** 98–101 (2006).
33. Rüger, N., Berger, U., Hubbell, S. P., Vieilledent, G. & Condit, R. Growth strategies of tropical tree species: disentangling light and size effects. *PLoS ONE* **6,** e25330 (2011).
34. Chave, J. *et al.* Tree allometry and improved estimation of carbon stocks and balance in tropical forests. *Oecologia* **145,** 87–99 (2005).
35. Sibly, R. M., Brown, J. H. & Kodric-Brown, A. (eds) *Metabolic Ecology: A Scaling Approach* (John Wiley & Sons, 2012).
36. Zanne, A. E. *et al.* Data from: Towards a worldwide wood economics spectrum. In *Dryad Digital Data Repository*, http://dx.doi.org/10.5061/dryad.234 (2009).
37. Enquist, B. J. & Niklas, K. J. Global allocation rules for patterns of biomass partitioning in seed plants. *Science* **295,** 1517–1520 (2002).

38. Niklas, K. J. Plant allometry: is there a grand unifying theory? *Biol. Rev.* **79,** 871–889 (2004).
39. Metropolis, N., Rosenbluth, A. W., Rosenbluth, M. N., Teller, A. H. & Teller, E. Equation of state calculations by fast computing machines. *J. Chem. Phys.* **21,** 1087–1092 (1953).
40. Rüger, N., Huth, A., Hubbell, S. P. & Condit, R. Determinants of mortality across a tropical lowland rainforest community. *Oikos* **120,** 1047–1056 (2011).
41. R Development Core Team. *R: A Language and Environment for Statistical Computing* (R Foundation for Statistical Computing, 2009).
42. Hilborn, R. & Mangel, M. *The Ecological Detective: Confronting Models with Data* (Princeton Univ. Press, 1997).
43. Chambers, J. Q., Dos Santos, J., Ribeiro, R. J. & Higuchi, N. Tree damage, allometric relationships, and above-ground net primary production in central Amazon forest. *For. Ecol. Manage.* **152,** 73–84 (2001).
44. Baskerville, G. L. Use of logarithmic regression in the estimation of plant biomass. *Can. J. For. Res.* **2,** 49–53 (1972).
45. Canham, C. D. *et al.* Neighborhood analyses of canopy tree competition along environmental gradients in New England forests. *Ecol. Appl.* **16,** 540–554 (2006).
46. Coates, K. D., Canham, C. D. & LePage, P. T. Above- versus below-ground competitive effects and responses of a guild of temperate tree species. *J. Ecol.* **97,** 118–130 (2009).
47. Pretzsch, H. & Biber, P. Size-symmetric versus size-asymmetric competition and growth partitioning among trees in forest stands along an ecological gradient in central Europe. *Can. J. For. Res.* **40,** 370–384 (2010).
48. Gómez-Aparicio, L., García-Valdés, R., Ruíz-Benito, P. & Zavala, M. A. Disentangling the relative importance of climate, size and competition on tree growth in Iberian forests: implications for forest management under global change. *Glob. Change Biol.* **17,** 2400–2414 (2011).
49. Das, A. The effect of size and competition on tree growth rate in old-growth coniferous forests. *Can. J. For. Res.* **42,** 1983–1995 (2012).
50. Zianis, D., Muukkonen, P., Makipaa, R. & Mencuccini, M. Biomass and stem volume equations for tree species in Europe. *Silva Fennica Monogr.* **4,** 1–63 (2005).

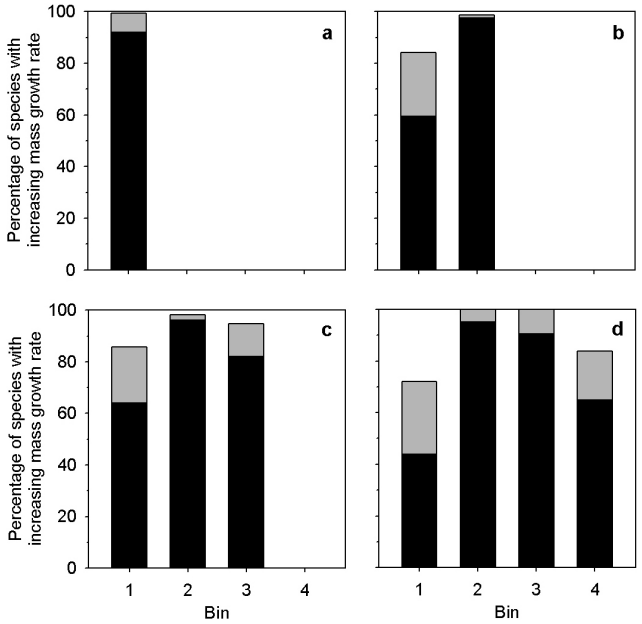

Extended Data Figure 1 | Summary of model fits for tree mass growth rates. Bars show the percentage of species with mass growth rates that increase with tree mass for each bin; black shading indicates percentage significant at $P \leq 0.05$. Tree masses increase with bin number. **a**, Species fitted with one bin (165 species); **b**, Species fitted with two bins (139 species); **c**, Species fitted with three bins (56 species); and **d**, Species fitted with four bins (43 species).

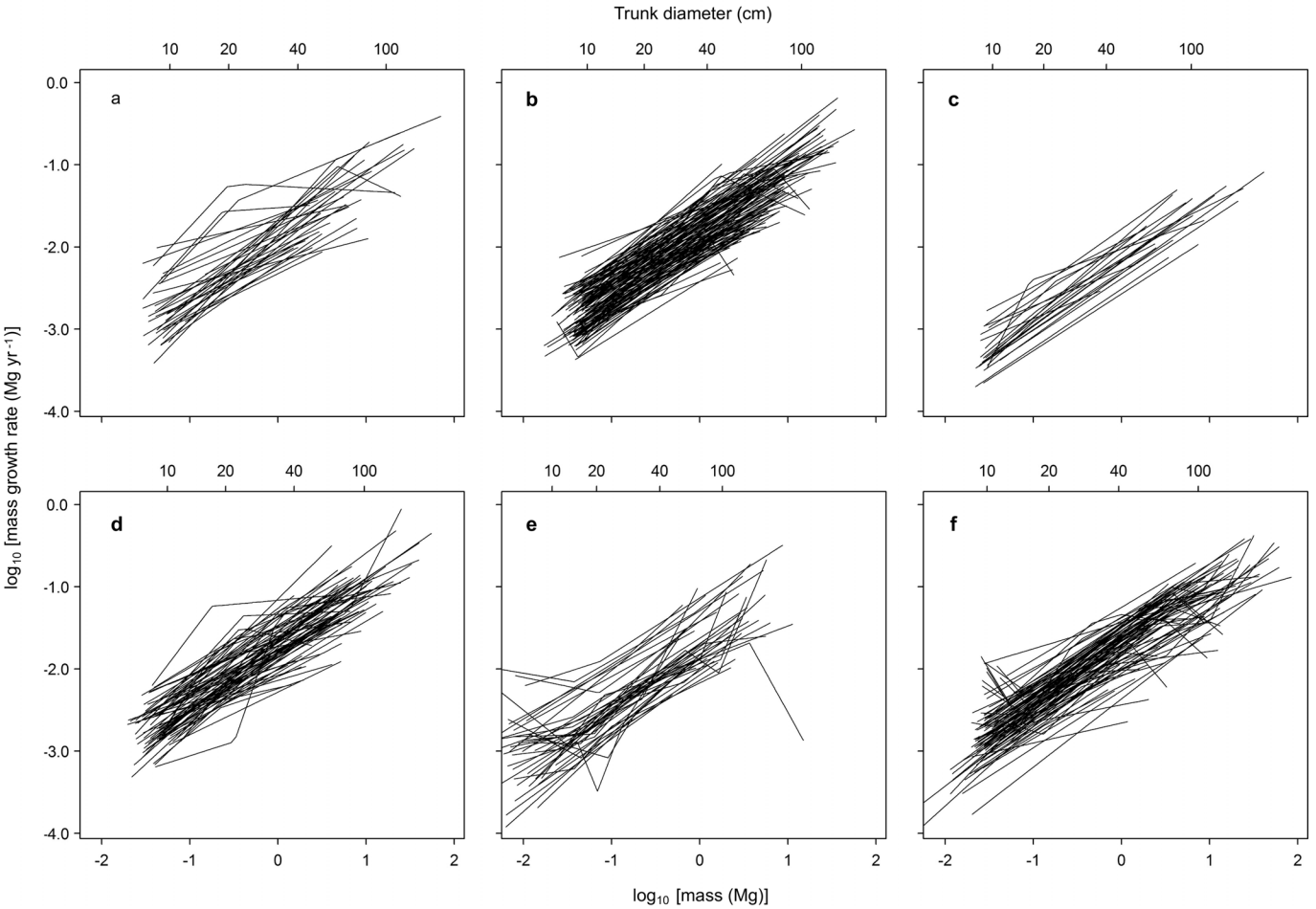

Extended Data Figure 2 | Log–log model fits of mass growth rates for 381 tree species, by continent. Trees with growth rates ≤ 0 were dropped from the analysis, reducing the number of species meeting our threshold sample size for analysis. **a**, Africa (33 species); **b**, Asia (123 species); **c**, Australasia (22 species); **d**, Central and South America (73 species); **e**, Europe (41 species); and **f**, North America (89 species). Trunk diameters are approximate values for reference, based on the average diameters of trees of a given mass.

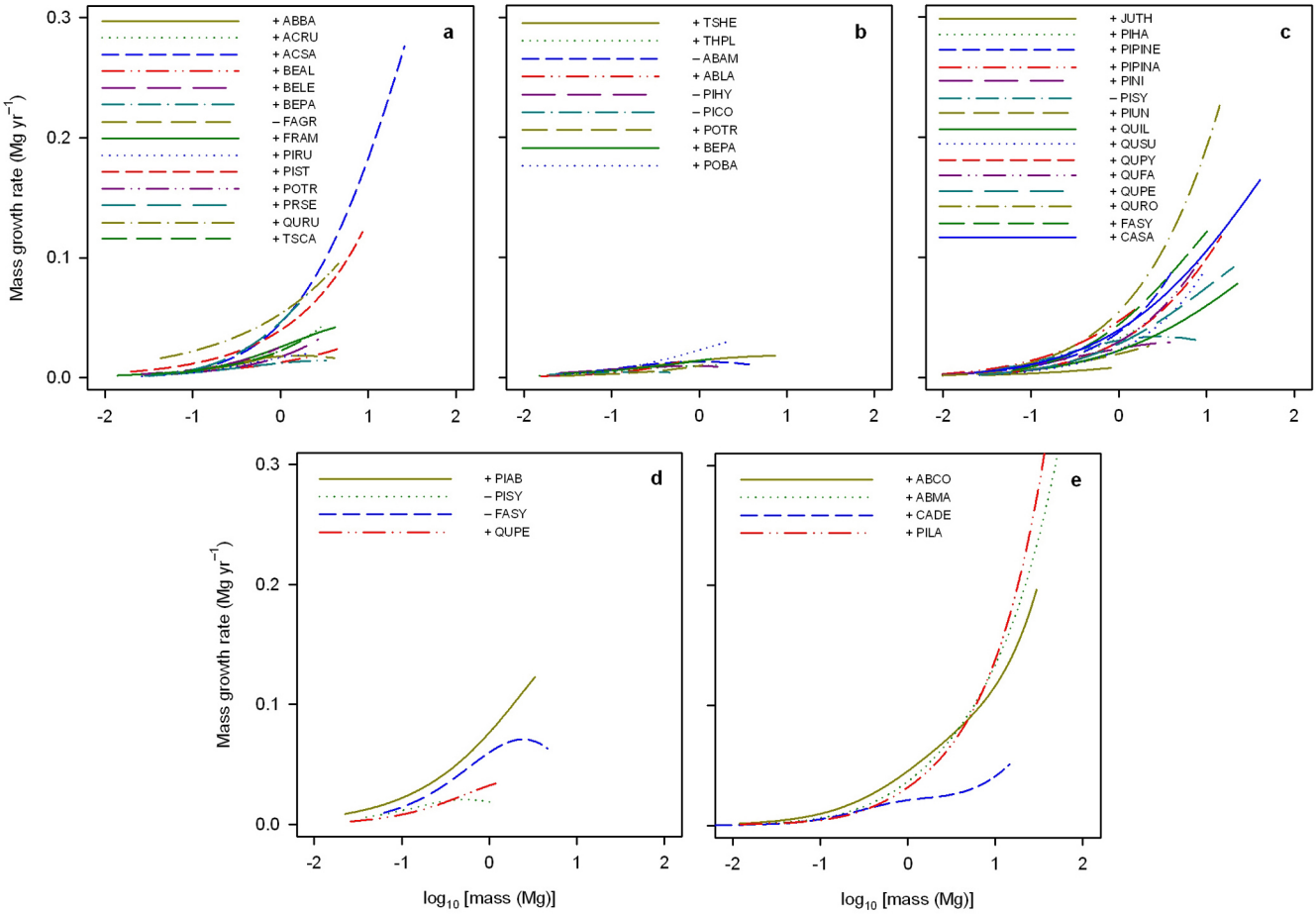

Extended Data Figure 3 | Aboveground mass growth rates for 41 tree species in the absence of competition. The '+' or '−' symbol preceding each species code indicates, respectively, species with mass growth rates that increased continuously with tree size or species with mass growth rates that declined in the largest trees. Sources of the diameter growth equations used to calculate mass growth were: **a**, ref. 45; **b**, ref. 46; **c**, ref. 48; **d**, ref. 47; and **e**, ref. 49. ABAM, *Abies amabilis*; ABBA, *Abies balsamea*; ABCO, *Abies concolor*; ABLA, *Abies lasiocarpa*; ABMA, *Abies magnifica*; ACRU, *Acer rubrum*; ACSA, *Acer saccharum*; BEAL, *Betula alleghaniensis*; BELE, *Betula lenta*; BEPA, *Betula papyrifera*; CADE, *Calocedrus decurrens*; CASA, *Castanea sativa*; FAGR, *Fagus grandifolia*; FASY, *Fagus sylvatica*; FRAM, *Fraxinus americana*; JUTH, *Juniperus thurifera*; PIAB, *Picea abies*; PICO, *Pinus contorta*; PIHA, *Pinus halepensis*; PIHY, *Picea* hybrid (a complex of *Picea glauca*, *P. sitchensis* and *P. engelmannii*); PILA, *Pinus lambertiana*; PINI, *Pinus nigra*; PIPINA, *Pinus pinaster*; PIPINE, *Pinus pinea*; PIRU, *Picea rubens*; PIST, *Pinus strobus*; PISY, *Pinus sylvestris*; PIUN, *Pinus uncinata*; POBA, *Populus balsamifera* ssp. *trichocarpa*; POTR, *Populus tremuloides*; PRSE, *Prunus serotina*; QUFA, *Quercus faginea*; QUIL, *Quercus ilex*; QUPE, *Quercus petraea*; QUPY, *Quercus pyrenaica*; QURO, *Quercus robar*; QURU, *Quercus rubra*; QUSU, *Quercus suber*; THPL, *Thuja plicata*; TSCA, *Tsuga canadensis*; and TSHE, *Tsuga heterophylla*.

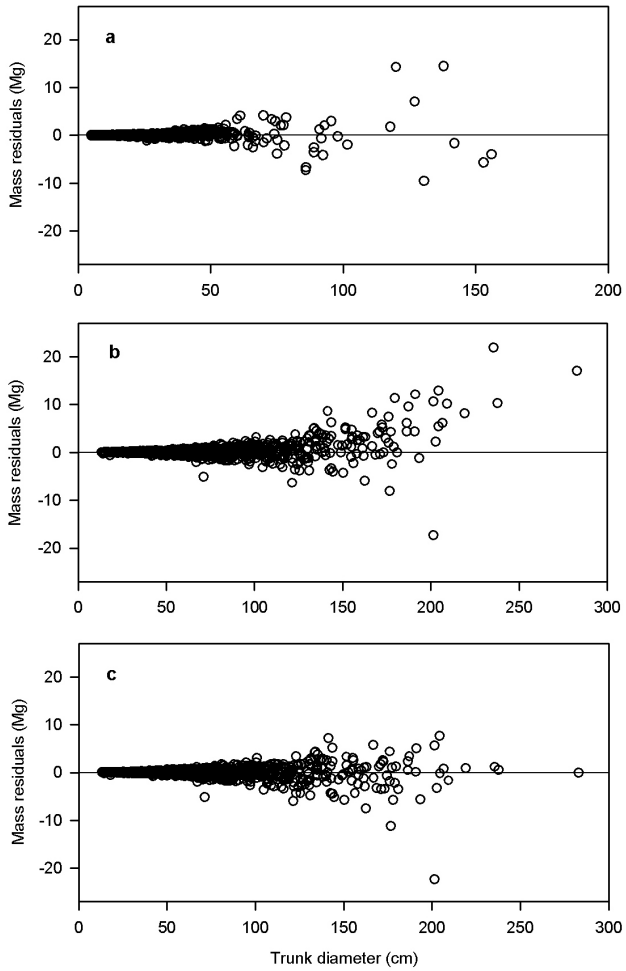

Extended Data Figure 4 | Residuals of predicted minus observed tree mass. **a**, The allometric equation for moist tropical forests[34]—used for the majority of tree species—shows no evident systematic bias in predicted aboveground dry mass, *M*, relative to trunk diameter ($n = 1{,}504$ trees). **b**, In contrast, our simplest form of allometric equation—used for 22% of our species and here applied to nine temperate species—shows an apparent bias towards overestimating *M* for large trees ($n = 1{,}358$ trees). **c**, New allometries that we created for the nine temperate species removed the apparent bias in predicted *M*.

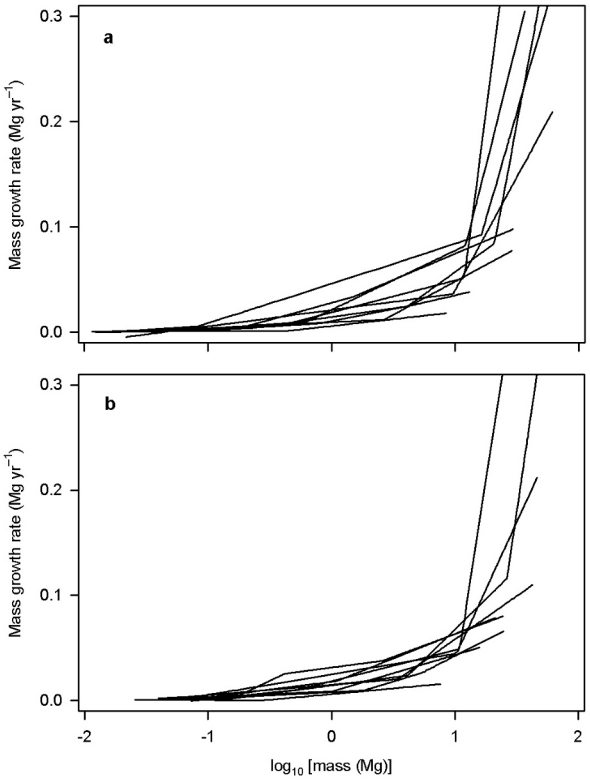

Extended Data Figure 5 | Estimated mass growth rates of the nine temperate species of Extended Data Fig. 4. Growth was estimated using the simplest form of allometric model [$\log(M) = a + b\log(D)$] (**a**) and our allometric models fitted with piecewise linear regression (**b**). Regardless of the allometric model form, all nine species show increasing G in the largest trees.